DEM analysis of the post-liquefaction shear deformation of sand

Analyse DEM de la déformation de cisaillement du sable post-liquéfaction

Rui Wang
Department of Hydraulic Engineering, Tsinghua University, China, wangrui_05@mail.tsinghua.edu.cn

Pengcheng Fu
Atmospheric, Earth, and Energy Division, Lawrence Livermore National Laboratory, USA

Jian-Min Zhang
Department of Hydraulic Engineering, Tsinghua University, China

Yannis F. Dafalias
Department of Civil and Environmental Engineering, University of California, Davis, USA; School of Applied Mathematical and Physical Sciences, National Technical University of Athens, Greece

ABSTRACT: In an effort to study the undrained post-liquefaction cyclic shear deformation of sand that has been observed in many undrained cyclic laboratory tests, the discrete element method (DEM) is adopted to conduct undrained cyclic biaxial simulations on granular assemblies consisting of 2D circular particles, successfully reproducing the generation and eventual saturation of shear strain amplitude at zero effective stress after initial liquefaction. DEM simulation tests show that conventional external and internal variables are found to be inadequate in describing and explaining the observations for post-liquefaction shear strain. A new fabric measure, the "Mean Neighboring Particle Distance" or *MNPD* is introduced based on observations of coordination number at liquefaction in DEM simulations and assessment of the structure of granular assemblies, which exhibits a strong unique correlation with the post-liquefaction shear strain, unravelling the micromechanical subtleties of the phenomenon.

RÉSUMÉ : Dans le but d'étudier la déformation cyclique de cisaillement non drainé de sable post-liquéfaction qui a été observée dans de nombreux essais cycliques non drainés au laboratoire, la Méthode des Éléments Discrets (DEM en anglais) est adoptée pour simulations biaxiales cycliques non drainées sur des assemblages granulaires constitués de particules circulaires 2D, et a reproduit avec succès la génération et éventuelle saturation de l' amplitude de la déformation de cisaillement à une contrainte effective nulle après la liquéfaction initiale. DEM simulations montrent que les variables conventionnelles externes et internes sont inadéquates pour décrire et expliquer les observations de cisaillement post-liquéfaction. On introduit une nouvelle mesure de structure, la « Distance Moyenne des Particules Voisines » (MNPD en anglais), basée sur des observations de nombre de coordination à la liquéfaction dans des simulations DEM et une évaluation de la structure des assemblages granulaires qui présente une forte corrélation unique avec la déformation de cisaillement post-liquéfaction, résolvant les subtilités micromécaniques du phénomène.

KEYWORDS: Liquefaction; DEM; Undrained cyclic loading; Post-liquefaction shear deformation; Fabric.

1 INTRODUCTION

Large but bounded shear strain has been observed in undrained cyclic tests on sand after the sample reaches initial liquefaction (e.g. Kutter et al., 1994; Zhang et al., 1997), as shown in Fig. 1. This post-liquefaction shear strain (γ_0, Zhang and Wang 2012) is an important contributing factor for the excessive deformation occurring during earthquakes. γ_0 has been observed to progressively increase in amplitude with increasing number of loading cycles, until it eventually stabilizes at a bounded saturated value γ_{0s}, even though the stress paths and the stress-strain relationship in the non-liquefaction states remain identical among the loading cycles.

Notwithstanding the frequent observation of the post-liquefaction shear deformation phenomenon in laboratory tests, a globally accepted explanation for this γ_0 has not been reached yet. Significant effort towards this end has been made in several constitutive studies (e.g. Zhang and Wang, 2012; Boulanger and Ziotopoulou, 2013; Wang et al., 2014). However, most current explanations still lack solid evidence to verify the assumptions that they introduce.

The current study aims to explain the generation of the large but bounded post-liquefaction shear deformation γ_0 by identifying a measureable variable with clear physical meaning able to quantify the fabric evolutions during post-liquefaction cyclic loading and shown to be correlated with γ_0.

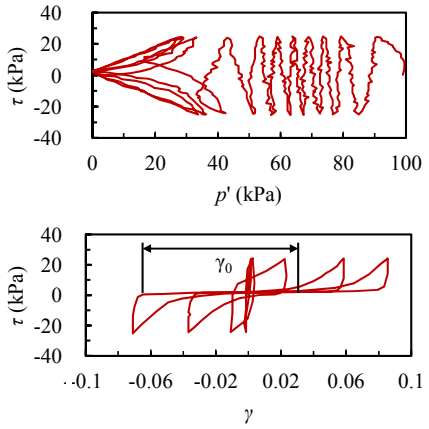

Figure 1. Undrained cyclic torsional test on Toyoura sand at D_r=48%. (Test data from Zhang et al. 1997).

2D discrete element method (DEM) (Cundall and Strack, 1979) is used in this study to simulate granular materials and

provide microscopic measurements that are very difficult or impossible to obtain in laboratory experiments with current technology. Several application of DEM in studying sand liquefaction have verified DEM's capability of reproducing the undrained cyclic behavior of sand (e.g. Ng and Dobry, 1994; Sitharam et al., 2009; Kuhn et al., 2014; Wang and Wei, 2016, Wang et al., 2016).

A 2D DEM simulation package *PPDEM* (Fu et al., 2012) is employed to conduct undrained cyclic biaxial simulations. Specimens for undrained cyclic biaxial simulations are first isotropically consolidated under initial effective mean stress p_{in}, and then undrained cyclic biaxial loading is achieved through controlling the velocities of the four walls enclosing the specimen, ensuring constant enclosed area by the four walls. Circular particles ranging from 0.30 mm to 1.00 mm in diameter are generated to fabricate polydispersed numerical specimens. The stress, void ratio, and fabric tensors within the specimens during the simulations can be measured as described by Wang et al. (2016).

2 γ_0 IN DEM SIMULATIONS AND ITS RELATIONSHIP WITH MACROSCOPIC QUANTITIES

2 .1 *Typical stress-strain results*

Fig. 2 shows the typical stress and strain results from a DEM undrained cyclic biaxial simulation on a specimen with void ratio of 0.191, with initial mean effective stress p_{in} of 100kPa and deviatoric stress amplitude q_{max} of 25kPa. Here, the deviatoric stress $q=(\sigma_1-\sigma_2)/2$, and the mean stress $p=(\sigma_1+\sigma_2)/2$, where σ_1 and σ_2 are the major and minor principal stress components, respectively. The stress path in Fig. 2 shows that the DEM results captures the cyclic behavior observed in laboratory tests (Fig. 1). More importantly for this study, it is shown that undrained cyclic biaxial DEM simulation is able to reproduce and confirm the generation and eventual saturation of post-liquefaction shear strain γ_0 (Fig. 1), through the deviatoric stress and shear strain relationship in Fig. 2.

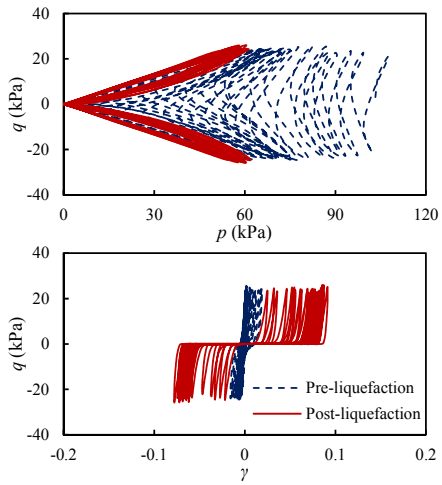

Figure 2. Typical DEM undrained cyclic biaxial simulation stress and strain result (specimen with void ratio of 0.191).

2 .2 *Conventional macroscopic quantities*

Upon confirming the ability to reproduce the post-liquefaction behavior of sand numerically using DEM, we are then able to investigate the influence factors and cause for the post-liquefaction shear strain γ_0.

First, the influence of external loading quantities on γ_0 is analyzed, including the initial mean effective stress p_{in} and the deviatoric stress amplitude q_{max}. Obviously, these two factors do not change from cycle to cycle, hence, they cannot reflect the increase of γ_0 with increasing load cycle. Fig. 3 shows the influence of these two factors on the saturated γ_{0s} for specimens with initial void ratio of 0.208 under 4 different q_{max} and 4 different p_{in}. We can see that there is not a significantly observable pattern of change in the γ_{0s} for the simulations with different q_{max} and p_{in}, all falling within the range of 0.215-0.225, which is a rather small range compared with the range of 0.045-0.391 shown in Fig. 4 for simulation on specimens with different void ratio and loading history. Thus, we can say that the post-liquefaction shear strain is independent of the initial mean effective stress and the deviatoric stress amplitude.

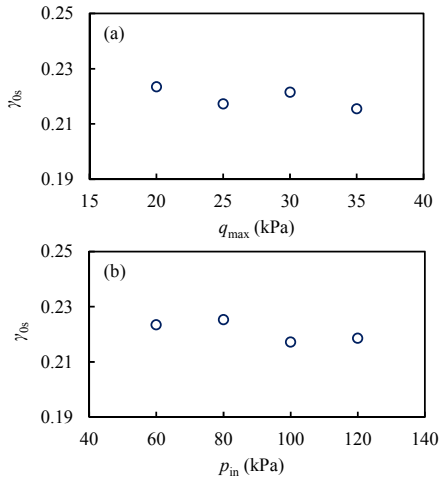

Figure 3. Influence of (a) shear stress amplitude q_{max} and (b) mean initial effective stress p_{in} on the saturated post-liquefaction shear strain γ_{0s} (specimens with initial void ratio of 0.208).

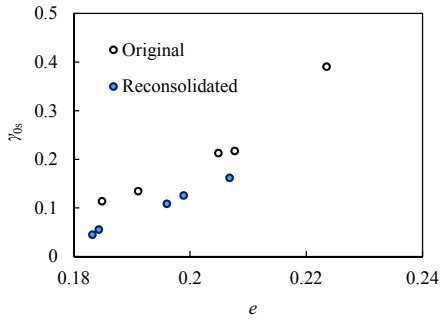

Figure 4. Relationship between specimen void ratio and the saturated post-liquefaction shear strain γ_{0s} in 10 different undrained cyclic biaxial simulations.

With the influence of the external loading quantities set aside, we then come to one of the most basic internal fabric quantities of sand, the void ratio e. Again, the void ratio does not change during undrained loading, hence, it cannot reflect the increase in γ_0 from cycle to cycle. To study the role of void ratio in the saturation of the post-liquefaction shear strain, undrained cyclic biaxial simulations are carried out on five specimens with different void ratios. γ_{0s} is observed to be significantly affected by the void ratio. When the γ_{0s} of these five tests are plotted in Fig. 4 with hollow markers, a positive correlation can be observed between γ_{0s} and void ratio. However, unfortunately, there is not a unique correlation between γ_{0s} and e. After completing these five undrained cyclic biaxial tests, the specimens are reconsolidated from a liquefied state and then undergo the same undrained cyclic biaxial loading again. The result of these undrained cyclic biaxial simulations on the reconsolidated samples are plotted in Fig. 4 using filled markers. It is clear that specimens with very

different void ratios could result in similar γ_{0s}, and vice versa, when compared to the results from the five original simulations.

3 A NEW FABRIC MEASUREMENT DETERMINING γ_0

3 .1 *Microstructure insight of sand liquefaction*

The inadequacy of conventional macroscopic measurements in describing the post-liquefaction shear strain motivates us to investigate other intrinsic quantities associated with this phenomenon. Fig. 5 plots the typical evolution of the coordination number C in undrained cyclic biaxial simulations. In all the 2D simulations conducted in this study, the coordination number C initiated at approximately 3 after isotropic consolidation, and as undrained cyclic loading continues, C decreases with increasing number of load cycles. Once C drops below approximately 2.2, the specimens reach initial liquefaction, and maintains a state of liquefaction when C is smaller than 2.2 in subsequent loading cycles. In conclusion the min of C reaches a stabilized level much before γ_0 does, hence, no correlation is possible.

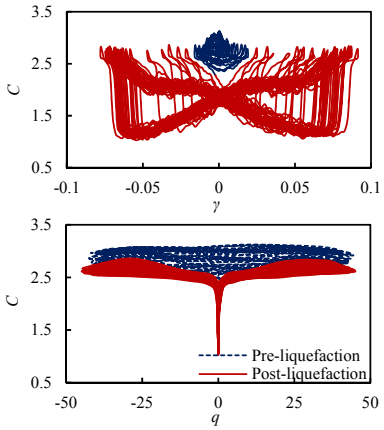

Figure 5. Evolution of coordination number C in an undrained cyclic biaxial simulation (specimen with void ratio of 0.191).

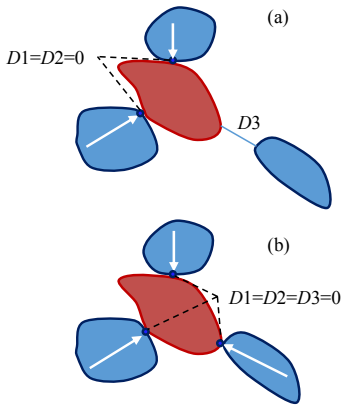

Figure 6. Sketch of the microstructure of neighboring particles: (a) a particle with two contacting particles, and (b) a particle with three contacting particles.

Observations of coordination number promote the consideration of the micromechanical structure of granular assemblies. For a 2D particle, if there are only 2 or fewer contacts, the particle would not be able to bear the contact forces stably, as shown in Fig. 6 (a). To stably bear contact load, at least 3 contacts are needed (Fig. 6 (b). This suggests that when the average contacts per particle in a granular assembly drops below a certain value, which is 2.2 in the simulations, the specimen loses its ability to form an effective load-bearing skeleton and liquefies.

The coordination number provides insights into the state of the granular material during liquefaction, where at a liquefaction state, the material is overall in a "fluid like" regime. The current coordination number tells how many more contacts, on a per-particle basis, the material needs to build a stable load-bearing structure. More directly related to γ_0 is the distance between each particle and its neighboring particles with which the contacts are necessary for constructing the skeleton.

3 .2 *Mean neighboring particle distance (MNPD)*

Based on this understanding of the micromechanical structure, the concept of "Neighboring Particle Distance" (*NPD*) is proposed to quantify the aforementioned particle distances in the "fluid like" regime. The *NPD* of a particle is defined as the mean surface-to-surface distance between this particle and its n closest neighboring particles, with n being the number of contacts needed to support a stable load-bearing structure, which is 3 in 2D. The mean value of *NPD* over all particles in a granular material is then a fabric characteristic or internal variable of the assembly that can be referred to as the *MNPD* (Mean Neighboring Particle Distance) and defined analytically by:

$$MNPD = \sum_{k=1}^{N}\sum_{i=1}^{n} Di^{k} / (nN) \qquad (1)$$

where N is the number of particles in the assembly, k is an index that runs over all the particles within the scope of analysis, and i is an index that runs over each particle's n closest neighboring particles. The *MNPD* is introduced with the notion to reflect the amount of particle rearrangement needed for a liquefied granular material to reach a load-bearing state, associating with the post-liquefaction shear strain γ_0.

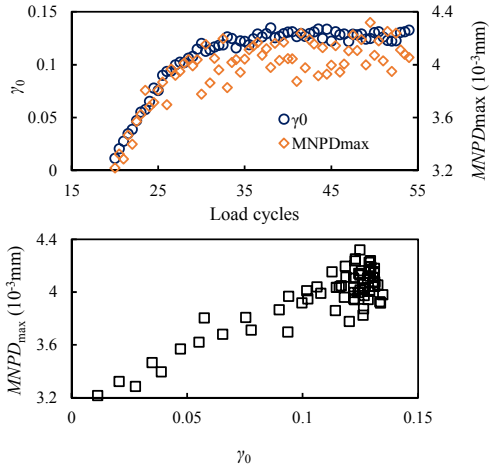

Figure 7. Development of the post-liquefaction shear strain γ_0 and the maximum neighboring particle distance $MNPD_{max}$ during each load cycle in an undrained cyclic biaxial simulation (specimen with void ratio of 0.191).

The development of the maximum value of the newly proposed *MNPD* fabric measurement in each load cycle is compared to the development of the post-liquefaction shear strain amplitude γ_0 in Fig. 7 for the simulation on a specimen with void ratio of 0.191. It can be observed that the $MNPD_{max}$ in each post-liquefaction cycle follows a highly similar trend of increase and saturation as that of γ_0, and there is a strong correlation between $MNPD_{max}$ and γ_0. This unique correlation of γ_0 with the $MNPD_{max}$ in each post-liquefaction cycle holds

true for all the simulations conducted in this study regardless of specimen initial states, loading conditions, and loading histories.

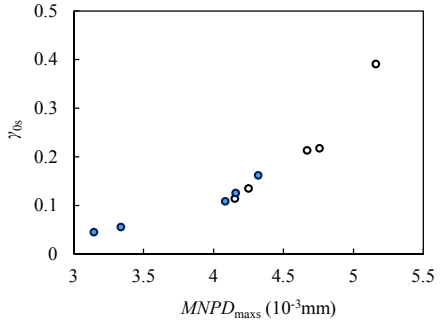

Figure 8. Dependency of the saturated post-liquefaction shear strain γ_{0s} on the saturated maximum neighboring particle distance $MNPD_{max}$ in 10 different undrained cyclic biaxial simulations.

Fig. 8 shows the relationship between the final saturated $MNPD_{maxs}$ and γ_{0s} values in the corresponding cycles in the 10 different simulations presented in this study. As the correlation between $MNPD_{max}$ and γ_0 of each load cycle suggests, a strong correlation exists between saturated $MNPD_{maxs}$ and γ_{0s} for all the void ratios and loading histories included. A comparison between Fig. 8 with Fig. 4 indicates that while the overall void ratio is the same, internal particle arrangement and structure of sand could be changed through different loading histories, and have significant influences on the behavior of sand. While γ_{0s} and void ratio e do not fall on the same line for the original and reconsolidated samples, the relationship between γ_{0s} and $MNPD_{maxs}$ is unique, irrespective of the load history, making *MNPD* a more appropriate fabric measurement than void ratio e in describing the undrained post-liquefaction cyclic shear strain.

4 CONCLUSION

Undrained cyclic biaxial DEM simulations on 2D circular particles is used in this study to reproduce and confirm the generation and eventual saturation of post-liquefaction shear strain γ_0, as observed in laboratory tests on sand. In showing that conventional fabric measurements are unable to provide a definitive correlation with shear strain development during cyclic liquefaction, a new fabric measurement is proposed based on observations of the micromechanical structure of granular material.

The new fabric measurement, Mean Neighboring Particle Distance (*MNPD*), is formulated to establish a definitive connection between post-liquefaction shear deformation development and a theoretically measurable intrinsic fabric metric. *MNPD* is introduced with the notion of reflecting the amount of rearrangement needed for a liquefied granular assembly to reach a stable load-bearing state, and unveils a new aspect of mechanical behavior of granular soils that traditional fabric measurements have largely overlooked, which is the internal arrangement of the particle and void system.

The current study employs 2D circular particles in the DEM simulations, which is a good way to reflect the core concepts of the post-liquefaction shear strain γ_0 and the mean neighboring particle distance *MNPD*. Further study using 3D complex shape particles would be a useful extension of the presented work.

Observations on the liquefaction susceptibility is also made during the DEM analysis showing that the number of undrained load cycles needed for a specimen to reach initial liquefaction is not solely determined by the void ratio or the current formulation for *MNPD*, and is strongly influenced by the liquefaction and reconsolidation history. More effort should be put into investigating this phenomenon, as it not only has significant theoretical value but is also extremely important in engineering practice, with the observation of liquefaction under a sequence of seismic events in several recent earthquakes.

5 ACKNOWLEDGEMENTS

The authors would like to acknowledge the National Natural Science Foundation of China (No. 51678346) for funding the work presented in this paper. The research leading to these results has received funding from the European Research Council under the European Union's Seventh Framework Program FP7-ERC-IDEAS Advanced Grant Agreement no. 290963 (SOMEF). Pengcheng Fu's contribution was performed under the auspices of the U.S. Department of Energy by Lawrence Livermore National Laboratory under Contract DE-AC52-07NA27344. This paper is LLNL report LLNL- CONF-716441. The authors would also like to thank Abudushalamu Aili for kindly translating the title and abstract of this paper into French. Part of this work was adopted from Wang et al. (2016, Acta Geotechnica) under the Creative Commons Attribution 4.0 International License (http://creativecommons.org/licenses/by/4.0/).

4 REFERENCES

Boulanger R.W., Ziotopoulou K. 2013. Formulation of a sand plasticity plane-strain model for earthquake engineering applications. *Soil Dynamics and Earthquake engineering* 53, 254-267.

Cundall P.A., Strack O.D.L. 1979. A discrete numerical model for granular assemblies. *Geotechnique* 29(1), 47-65.

Fu P., Walton O.R., Harvey J.T. 2012. Polyarc discrete element for efficiently simulating arbitrarily shaped 2D particles. *International Journal for Numerical Methods in Engineering* 89(5), 599-617.

Kuhn M.R., Renken H.E., Mixsell A.D., Kramer S.L. 2014. Investigation of Cyclic Liquefaction with Discrete Element Simulations. *Journal of Geotechnical and Geoenvironmental Engineering* 140(12), 04014075-1-13

Kutter B.L., Chen Y., Shen C.K. 1994. Triaxial and torsional shear test results for sand., *Naval Facilities Engineering Service Center, Contact Report CR 94.003-SHR*, Port Hueneme, California.

Ng T.T., Dobry R. 1994. Numerical simulations of monotonic and cyclic loading of granular soil. *Journal of Geotechnical Engineering* 120(2), 388-403.

Wang R., Fu P., Zhang J.M., Dafalias Y. 2016. DEM study of fabric features governing undrained post-liquefaction shear deformation of sand. *Acta Geotechnica* 11 (6), 1321-1337.

Wang R., Zhang J.M., Wang G. 2014. A unified plasticity model for large post-liquefaction shear deformation of sand. *Computers and Geotechnics* 59, 54-66.

Wang, G. and Wei, J., 2016. Microstructure evolution of granular soils in cyclic mobility and post-liquefaction process. *Granular matter* 18(3), 1-13.

Zhang J.M. and Wang G. 2012. Large post-liquefaction deformation of sand, part I: physical mechanism, constitutive description and numerical algorithm. *Acta Geotechnica* 7(2), 69-113.

Zhang J.M., Shamoto Y., Tokimatsu K. 1997. Moving critical and phase-transformation stress state lines of saturated sand during undrained cyclic shear. *Soils and Foundations* 2(37), 51-59.